

# A Method for Assessing the Effect of Polymer Sheeting Rheology, Surface Pattern, and Processing Conditions on Glass Lamination

YI-JE JUANG,<sup>1</sup> DENITRA BRUER,<sup>1</sup> L. JAMES LEE,<sup>1</sup> KURT W. KOELLING,<sup>1</sup> NARAYANAN SRINIVASAN,<sup>2</sup> CHARLES H. DRUMMOND,<sup>2</sup> BERT C. WONG<sup>3</sup>

<sup>1</sup> Department of Chemical Engineering, Center for Advanced Polymer & Composite Engineering, The Ohio State University, 125 Koffolt Labs., 140 W. 19th, Columbus, Ohio 43210 USA

<sup>2</sup> Department of Materials Science and Engineering, The Ohio State University, Columbus, Ohio 43210 USA

<sup>3</sup> DuPont Glass Laminating Products, P. O. Box 1217, Parkesburg, West Virginia 26102 USA

*Received 6 March 2000; accepted 27 June 2000*

**ABSTRACT:** An apparatus has been constructed wherein the transparency of a glass/polymer sheet/glass assembly undergoing vacuum de-airing can be monitored continuously. Experimental conditions can be varied independently, such as vacuum level, cold (ambient) de-airing time, and oven temperature. The behavior of polyvinyl butyral and an ionomeric interlayer (SGP) with different rheological properties and surface roughness were studied using various de-airing conditions. Initial results show that the clarity of the assembly is a monotonically increasing function of time in the oven at a given vacuum level. All assemblies made from these interlayers became clear with sufficient vacuum time at ambient temperature. The assembly from polyvinyl butyral with protrusion-type surface pattern clears up faster than that with indentation-type. © 2001 John Wiley & Sons, Inc. *J Appl Polym Sci* 80: 521–528, 2001

**Key words:** glass lamination; polyvinyl butyral; vacuum de-airing process; laminated safety glass

## INTRODUCTION

Laminated safety glass consists of a polymeric sheeting sandwiched between two plies of float glass. In automotive windshields, the thickness of each ply of glass is typically 2 mm, and that of the polymeric interlayer (e.g., polyvinyl butyral, PVB) is nominally 0.76 mm. PVB sheeting is commercially available in roll form. Roughness is im-

parted on the surface of the sheeting either by embossing or by melt fracture so as to prevent blocking while in storage or in shipment. In the fabrication of windshields, the glass and the PVB layers are assembled in an environmentally and cleanliness controlled area. The excess PVB sheeting is trimmed off. The assembly normally appears hazy, practically opaque, because of the surface roughness of the interlayer. Air in the interstices is removed by either sending the assembly after heating through sets of nip rolls, or by vacuum followed by heating. In both cases, the edges of the assembly are sealed at the end of this step. The assembly at this time is called a pre-press, and is generally clearer than when the

---

*Correspondence to:* L. J. Lee.  
Contract grant sponsor: DuPont Glass Laminating Products.

*Journal of Applied Polymer Science*, Vol. 80, 521–528 (2001)  
© 2001 John Wiley & Sons, Inc.

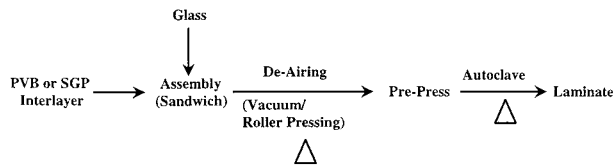


**Figure 1** Glass lamination process.

layers are first assembled. The pre-press is then heated to 135–150°C under pressure (8–15 bar) in an autoclave to remove all of the remaining haziness. A schematic for the glass lamination process is shown in Figure 1.

Various studies have been performed to investigate the properties of the polymer interlayer and the laminated glass. Vallabhan et al.<sup>1</sup> performed a direct-shear test to determine the shear deformation characteristics of PVB and concluded that, under very low strain rates, the shear modulus of the PVB interlayer depends on the amount of the total average shear strain in the interlayer, not on its thickness. Ellis and Lim<sup>2</sup> reported the observations of the Mullins type effect (stress-softening) that occurred when stretching the PVB interlayer and strain hardening happened beyond a critical strain,  $\epsilon_c$ . Both the amount of stress-softening and the critical strain were observed to depend on strain rate. Safy El-Din and Sabaa<sup>3</sup> conducted a series of experiments such as thermal degradation, viscosity, infrared, and contact angle measurements. They stated that the thermal treatment has a great effect on the chemical structure of PVB with a large reduction of hydroxyl and acetate groups and complete disappearance of the cyclic acetal groups. They also proposed a probable mechanism for thermal degradation of PVB.

As to the laminated glass, Behr et al.<sup>4</sup> and Vallabhan et al.<sup>5,6</sup> conducted several experiments regarding the laminated glass units under uniform lateral pressure. Huntsberger<sup>7</sup> studied the relationship between adhesion and performance of the laminated glass. David and Wittberg<sup>8</sup> performed peeling tests for the laminated glass and examined the surface. Sha et al.<sup>9</sup> performed the tension adhesion test to characterize the samples with three different levels of adhesion and analyzed the test results by using a micromechanical model of debonding for the glass/interlayer interface.

Other related studies can be found in the literature. Decker and Moussa<sup>10</sup> developed ultraviolet-curable resins for photocuring to produce lam-

inated glass. dos Reis<sup>11</sup> described an acousto-ultrasonic nondestructive method to evaluate laminated glass. Jandeleit<sup>12</sup> reported the improved properties of glass–plastic combinations. Shabanova et al.<sup>13</sup> introduced several methods for checking the optical distortion and image splitting properties of safety glass. Timmermann<sup>14</sup> described the instrument and methods to take the direct measurement of scattered light on the windshield, which can be used for inspection of the windshield.

Unlike the above studies, the pre-press quality attributed from the properties of the polymeric interlayer and the vacuum de-airing processing conditions have not been studied extensively. The residual haziness in the pre-press is viewed by some as evidence that much air is entrapped between the glass and polymer sheet. Recently, it has been observed that pre-presses with up to 70% haze have similar levels of entrapped air as pre-presses with 20% haze.<sup>15</sup> In most vacuum de-airing systems, it is not possible to observe how the transparency of an assembly changes as it travels through the system. It was, therefore, an objective of this study to develop an apparatus with which to study the change in transparency of the assembly in a vacuum de-airing system. It was a further objective of this study to use such an apparatus to study the behavior of PVB interlayers and a new ionomeric material, SGP, with different rheology and surface roughness in various de-airing conditions, and to assess the relative contribution of each to pre-press clarity.

## EXPERIMENTAL

### Vacuum De-Airing Apparatus

Figure 2(a) shows the schematic of the vacuum de-airing apparatus. It consists of a rectangular box with the dimensions 38 × 38 × 15 cm (15" × 15" × 6"). The sides of the box are made of stainless steel sheet whereas the walls are made of glass. The top and the bottom are also made of stainless steel sheet. The top has a slot for thermocouples and vacuum connections. Temperature control is achieved by two heat guns with feedback temperature controllers. The test sample is composed of two 30 × 30 cm (12" × 12") annealed glass plates with PVB (or SGP) sheeting in between. A rubber gasket with a tube extending as an outlet to pull vacuum is placed around the glass/interlayer/glass assembly. An aligned light

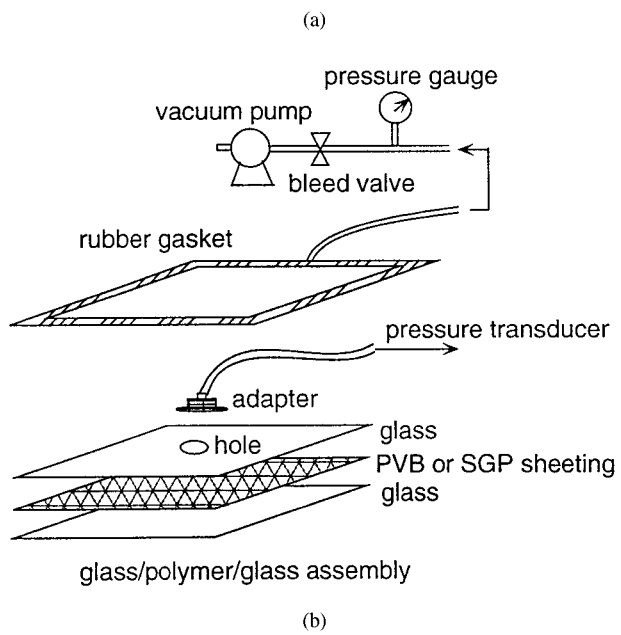
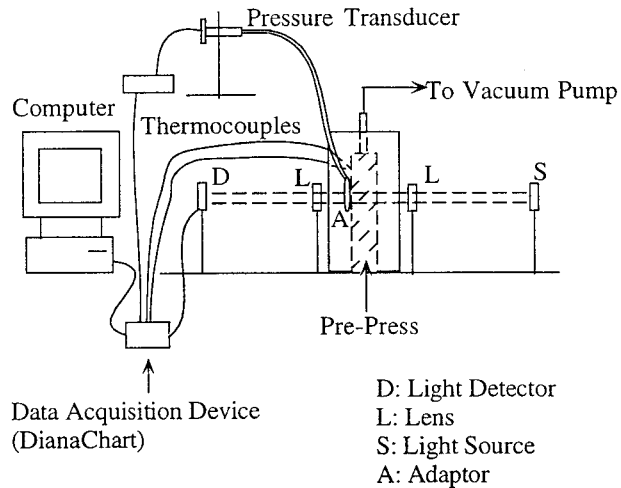


**Figure 2** (a) A schematic of de-airing apparatus, and (b) setup for interstitial pressure measurement.

source and a light sensor are placed which can convert the light transmission into electrical signals. The change of light transmission can then be measured as a function of processing time. The temperature of the pre-press is also measured. For the interstitial pressure measurement, a hole with 0.03-m diameter is drilled at the center on one side of the glass of the assembly, as shown in Figure 2(b). An adapter is mounted on the hole with its edge sealed. The adapter is then connected to a pressure transducer (model no. PX605-30VACI; OMEGA, Stamford, CT) which can measure negative pressure from 0 to 0.1 MPa (0 to 30" Hg vacuum). The interstitial pressure is

again monitored as a function of time. All data are recorded by a data acquisition system.

**Materials**

Seven different PVB sheeting (A1, A2, B1, B2, B3, B4, and C) classified into three groups (A,  $M_w$

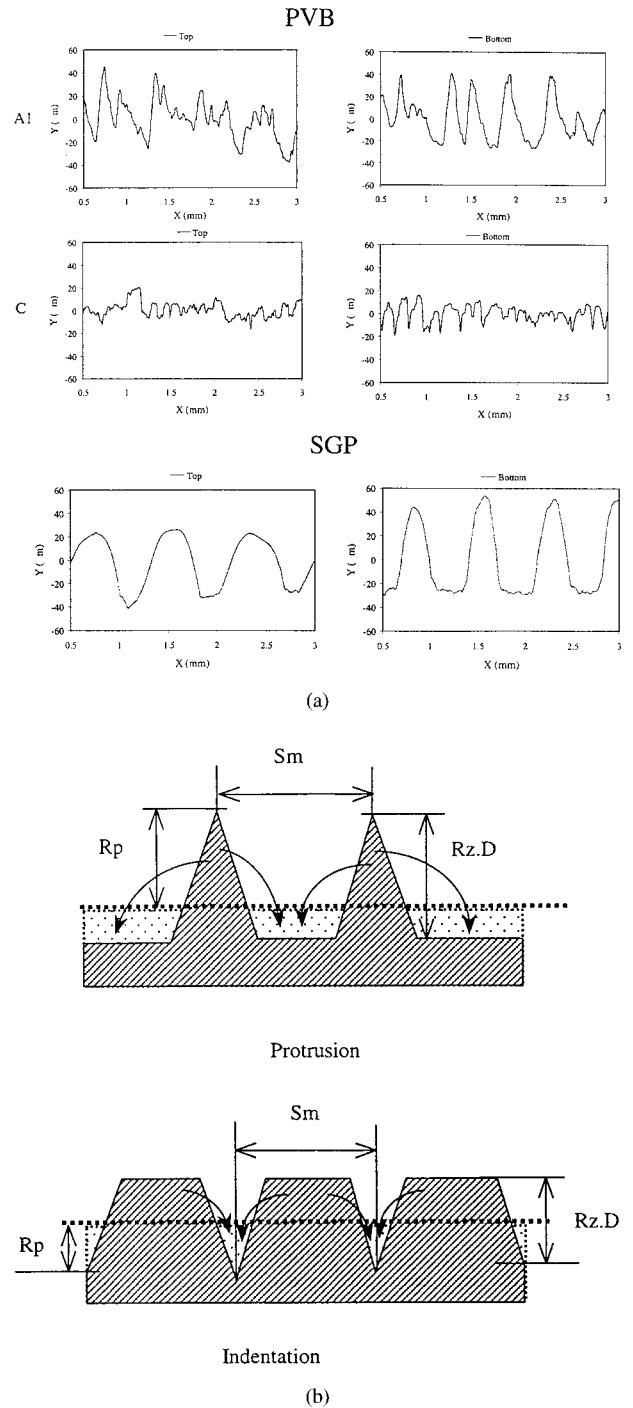


**Figure 3** (a) Actual surface profile, and (b) average surface profile of PVB and SGP sheeting.

**Table I Surface Roughness Parameters of PVB and SGP Sheeting**

Material	A1	A2	B1	B2	B3	B4	C	SGP
Top Rz.D ( $\mu\text{m}$ )	83.2	62.8	59.2	50.2	44.8	21.4	45.0	55.4
Bottom Rz.D ( $\mu\text{m}$ )	90.6	50.0	61.8	53.4	40.8	22.8	55.4	93.8
Top Sm ( $\mu\text{m}$ )	44.0	61.6	27.5	35.4	25.6	32.0	19.5	201
Bottom Sm ( $\mu\text{m}$ )	38.0	42.0	35.3	40.9	23.6	35.8	18.9	186.9

150,000; B,  $\bar{M}_w$  143,000; C,  $\bar{M}_w$  144,000), and a new ionomeric material, SGP, were used to study the effect of polymer rheology and surface pattern on glass lamination. The glass transition temperature is around 15°C for PVB and around 43°C for SGP. PVB sheeting was produced by melt fracture during extrusion, whereas SGP was produced by hot embossing. This results in the PVB exhibiting an irregular surface pattern whereas the SGP has a regular surface pattern. Figure 3(a) shows the actual surface pattern of PVB and SGP sheeting. For simplicity, several average-quantity terms are used to describe the surface roughness and pattern. They are shown in Table I and Figure 3(b). For PVB sheeting, both the top and the bottom surface patterns are random, but the average roughness is similar. The average peak height (Rz.D) ranges from 20 to 80  $\mu\text{m}$  and the average spacing of roughness peaks (Sm) ranges from 20 to 50  $\mu\text{m}$ . For SGP, however, the top and the bottom surface patterns are quite different from each other. The SGP sheeting was produced by embossing, in which different surface pattern and roughness were imparted on each side of the sheeting. The Rz.D of the top surface is 55.4, and that of the bottom is 93.8  $\mu\text{m}$ . Sm is 201, and 186.9  $\mu\text{m}$  for the top and bottom, respectively. Groups A and B of PVB and SGP have the protrusion type of surface pattern, whereas group C of PVB has the indentation type of surface pattern.

### Rheology Measurement

Because the melting of the surface pattern must partly be dependent on the interlayer's rheology, rheological properties of the interlayers were characterized by using a Rheometrics Mechanical Spectrometer, RMS-800, to measure the temperature and frequency dependent dynamic complex viscosity. The sample was made into a disk shape with 25-mm diameter, which is the same diameter as the parallel plates used in the study. It was then placed between two parallel plates, and

heated up to 140°C. After being slightly compressed to eliminate the surface-pattern roughness and squeeze out the trapped air, the sample was cooled down to the test temperature. The measurement was not initiated until the sample reached a thermal equilibrium. The test temperature ranged from 25 to 125°C and the frequency ranged from 0.01 to 100 Hz. The strain was held constant at 1%. The gap between the two plates was approximately 1 mm.

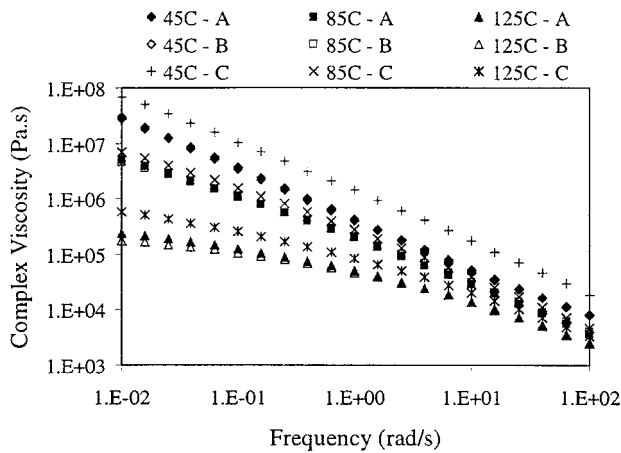
### Vacuum Pre-Pressing

The assembly with a polymeric interlayer between two plies of glass was surrounded by a rubber gasket, which was connected to a vacuum pump. The maximum voltage correlating to the highest light transmission was recorded before the assembly was placed in the thermal chamber. The assembly then underwent 7 min of vacuum de-airing at room temperature, followed by heating. The vacuum pump and heat guns were turned off after 30 min. Processing variables studied included the maximum oven temperature set point (120 and 135°C) and the vacuum level 53 and 80 kPa (16 and 24" Hg). The measured variables were light transmission and glass temperature as a function of time.

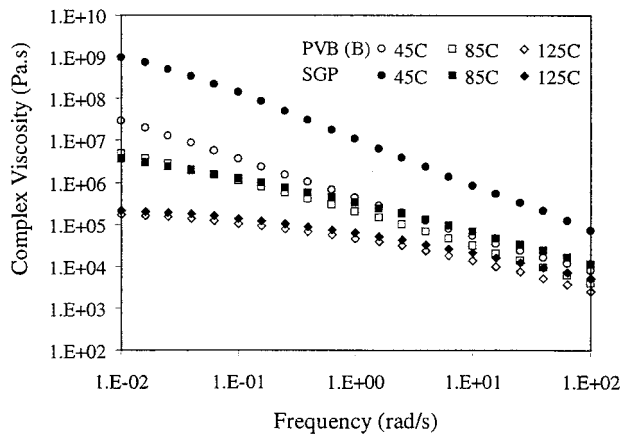
## RESULTS AND DISCUSSION

### Rheological Characterization

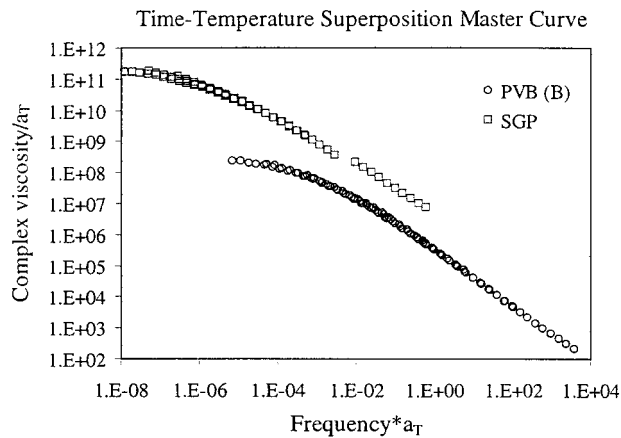
Figure 4(a) shows the complex viscosity vs frequency for three groups of PVB interlayers. Despite the different molecular weights, the complex viscosity is almost the same except that group C has a slightly higher viscosity. The comparison between SGP and PVB (B) is shown in Figure 4(b). At 85 and 125°C, SGP and PVB show very similar shear viscosity. At 45°C, the complex viscosity of SGP is approximately forty times larger than that of PVB. This is because the glass tran-



(a)



(b)



(c)

**Figure 4** Comparison of complex viscosity between (a) three different groups of PVB sheeting, (b) PVB and SGP sheeting, and (c) master curves of PVB and SGP sheeting at 65°C reference temperature.

sition temperature of SGP is around 43°C whereas it is 15°C for PVB, i.e., SGP has a more solid-like behavior than PVB at 45°C. The time-temperature-superposition master curves based on 65°C for PVB and SGP are shown in Figure 4(c). Both materials follow the WLF equation, with  $C_1 = 11.8, 6.8, C_2 = 168.9, 10.2$  for PVB and SGP, respectively.

**Vacuum Pre-Pressing**

The typical light transmission curves for PVB and SGP sheeting during de-airing are shown in Figure 5. For PVB, the curve can be divided into five different regions, i.e., the initial plateau, first transition, rapid-change, second transition, and final plateau regions. There are two differences between PVB and SGP curves. One is that there is not a clear first-transition region in the SGP light-transmission curve. Unlike PVB sheeting, SGP sheeting has a regular surface pattern and the air pockets formed between SGP sheeting and the glass is almost the same everywhere. Once the temperature reaches to around 65°C, every air pocket between SGP sheeting and the glass starts to collapse at the same time, leading to a sharp change of light transmission. The other difference is that the period of the second-transition region for SGP sheeting is shorter than that for PVB sheeting. Again, because of the regular surface pattern of SGP sheeting, the air pathway can remain almost clear throughout the entire

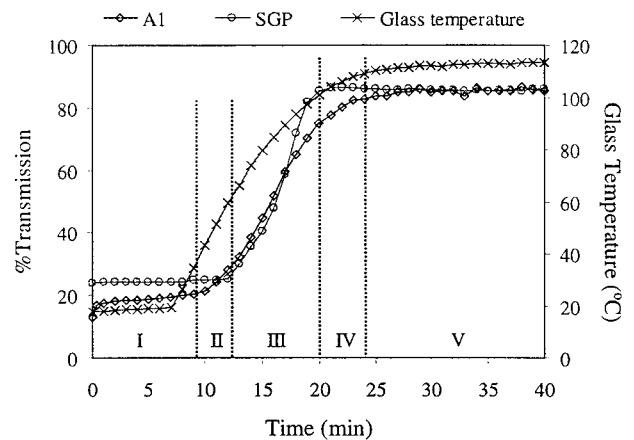


**Figure 5** The typical light transmission curves for PVB and SGP sheeting during de-airing (120°C oven temperature set point and 24" Hg vacuum level). I, Initial plateau region; II, first transition region; III, rapid-change region; IV, second transition region; and V, final plateau region.



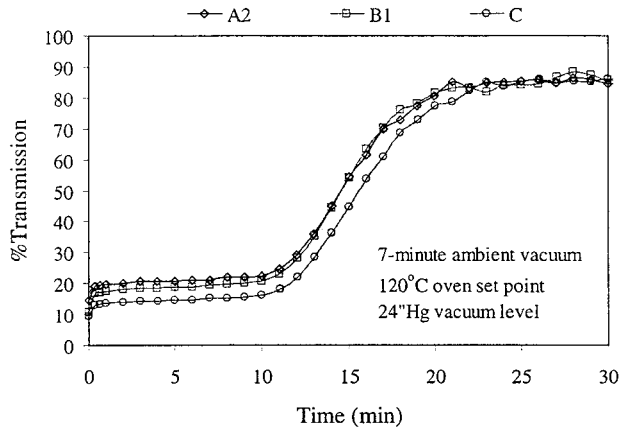


**Figure 6** The effect of surface pattern on light transmission.

de-airing process. This provides the highest compression force induced by vacuum (because of the lowest interstitial pressure), resulting in less time required in the second-transition region. The above results imply that SGP sheeting is more efficient than PVB sheeting in de-airing.

It is difficult to relate the light transmission to the surface roughness and pattern. Generally, the higher the Rz.D, the less transparent the sample will be before de-airing. However, the sample with a larger  $S_m$  may be more transparent because a larger  $S_m$  means a larger distance between two peaks, allowing more light to penetrate through the sample. Other parameters such as  $R_p$ , etc., may also contribute to light transmission. The sample with a protrusion type of surface pattern or a more regular surface pattern tends to have a higher light transmission than that with an irregular and indentation type of surface before de-airing. This might be attributed to the more severe light deflection for the later case.

#### Comparison Between Different Surface Pattern, Roughness, and Processing Conditions

Figure 6 shows the effect of surface pattern on light transmission with 7-min ambient vacuum before heating. The three sheeting samples compared have similar Rz.D but substantially different  $S_m$ . Furthermore, samples A2 and B1 have about the same viscosity, whereas sample C has a slightly higher viscosity. Sample C has indentation-type surface pattern whereas the other two have protrusion-type surface pattern. Sample C has the lowest initial light transmission among the three samples because the indentation-type

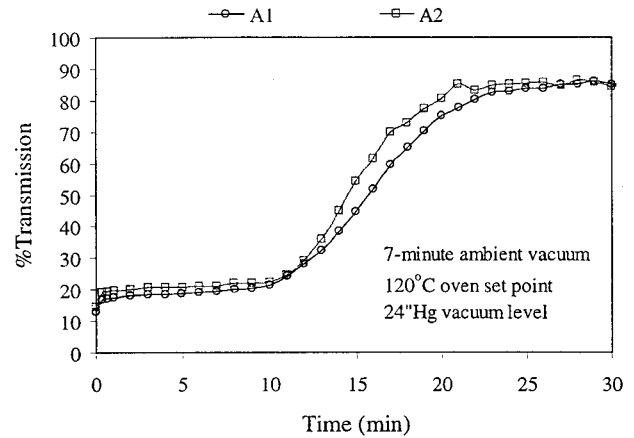


**Figure 7** The effect of surface roughness (Rz.D) on light transmission.

surface pattern may cause more absorption and deflection of light when it penetrates through the interlayer. For the light transmission change, all three samples follow the same pattern except that samples A2 and B1 clear up sooner. This could be a result of viscosity and surface-pattern differences.

Figure 7 shows a comparison of the data from PVB interlayers with the same molecular weight. In this comparison, sample A2 cleared up sooner than sample A1, because A2 is significantly rougher than A1 (29 Rz.D units). Figure 8 compares the results from two sheeting samples, B2 and B3, which have similar molecular weight and surface-roughness peak height (Rz.D) but the mean spacing is quite different ( $S_{mB2} > S_{mB3}$ ). Sample B2 has a higher initial light transmission

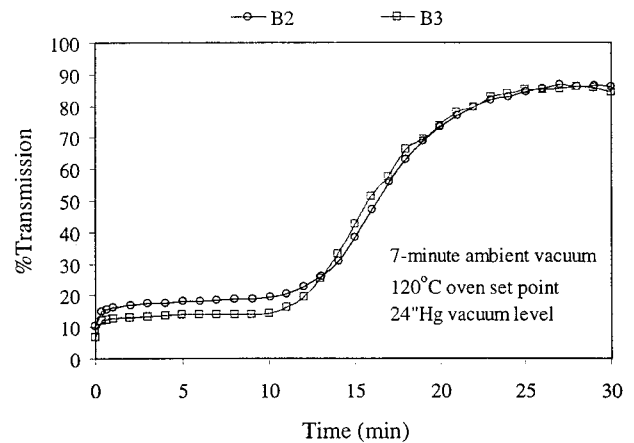


**Figure 8** The effect of roughness spacing ( $S_m$ ) on light transmission.

than B3, but there is little difference in their behavior during de-airing.

The comparison of the light transmission vs time between samples A1, B4, and SGP sheeting is shown in Figure 9, with 7-min ambient vacuum before heating. Sample B4 has the lowest surface roughness and the highest initial light transmission. The increase of light transmission of SGP occurs later, i.e., at a higher temperature. However, it clears up sooner than the other two PVB sheeting.

Figure 10(a, b, and c) shows the effect of processing conditions on light transmission for A1, B1, and B4, respectively. From these results, we observe that the sample will clear up sooner under a higher temperature set point and a higher vacuum level. For samples with a larger surface roughness, i.e., samples A1 and B1, the effect of vacuum level is more pronounced than that of temperature. However, for samples with a low surface roughness, i.e., sample B4, the difference between temperature and vacuum level effect on the de-airing is small.

Figure 11 shows the effect of processing conditions on light transmission of SGP. Although SGP sheeting has a large surface roughness, the vacuum level does not affect the de-airing much except in the beginning. This may be attributed to the large Sm value and the regular surface pattern (i.e., the interstitial pressure is not affected by vacuum). The higher temperature set point makes the sample clear up sooner.

CONCLUSION

An apparatus for observing the change in transparency in a pre-press during vacuum de-airing

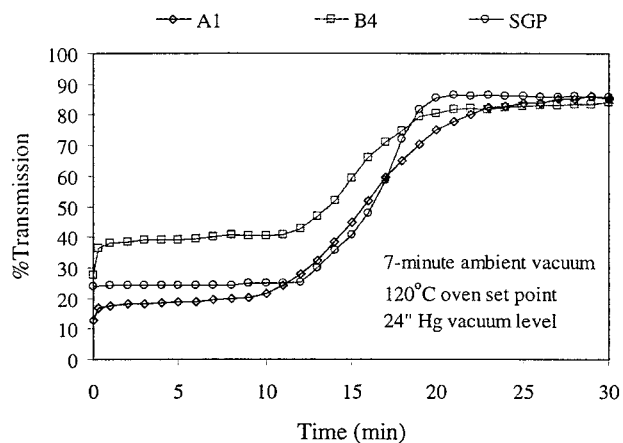


Figure 9 Comparison of light transmission between samples A1, B4, and SGP.

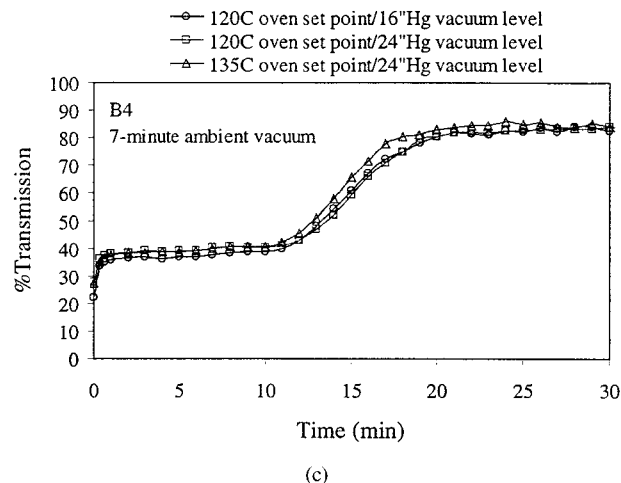
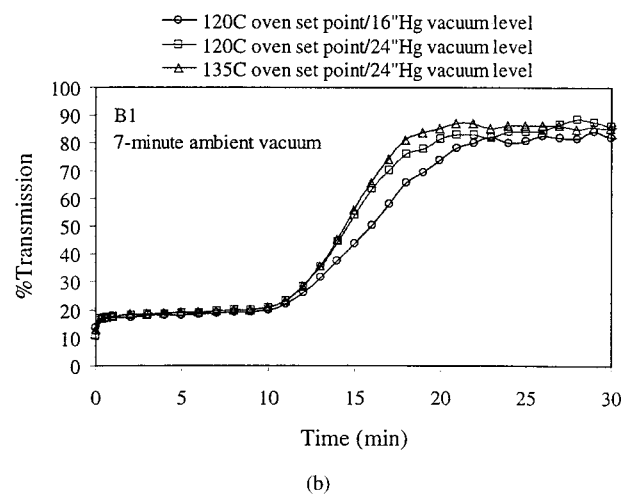
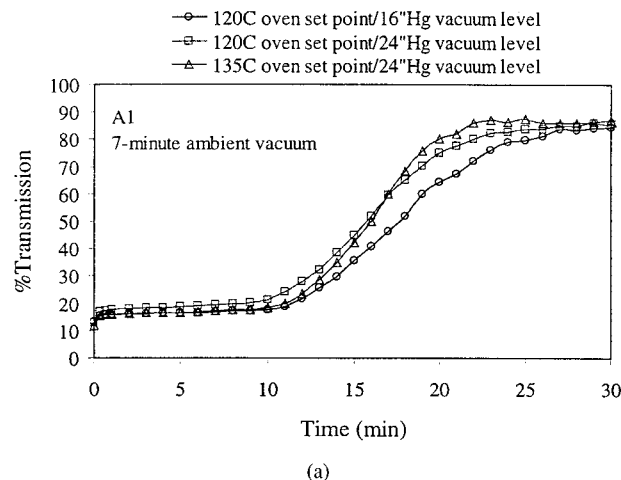
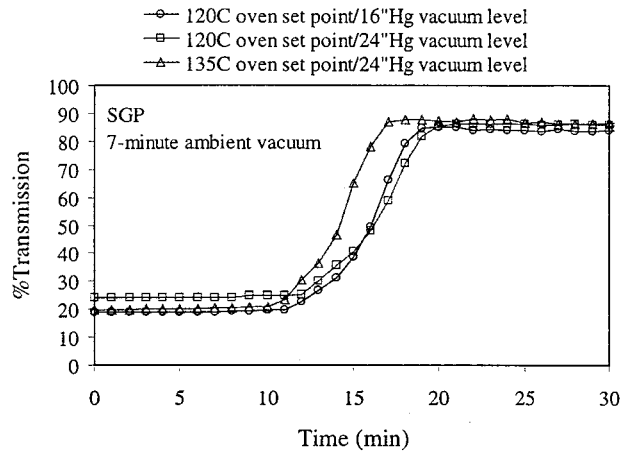


Figure 10 The effect of processing conditions on light transmission for (a) sample A1, (b) sample B1, and (c) sample B4.

in glass lamination has been developed. A method for studying the behavior of various PVB inter-layers in such a setup has also been discussed.



**Figure 11** The effect of processing conditions on light transmission for SGP.

This apparatus and the experimental method allow us to study the relative contributions of material properties such as rheology, surface roughness, surface pattern, and processing conditions on the clarity of the pre-press. Preliminary results show that with sufficient vacuum time at ambient temperature, all assemblies made from all PVB interlayers with roughness ranging from 20 to 80 microns become clear. The same conclusion can be made for SGP sheeting. Also, pre-presses from PVB sheeting with surface roughness of the protrusion type appear to clear up faster than that from the indentation type. Between PVB and SGP sheeting, SGP always clears up sooner.

The authors thank DuPont Glass Laminating Products (Parkersburg, WV) for financial support and material supply.

## REFERENCES

- Vallabhan, C. V. G.; Das, Y. C.; Ramasamudra, M. *J Mater Civil Eng* 1992, 4, 71.
- Ellis, B.; Lim, B. C. *J Mater Sci Lett* 1984, 3, 620.
- Safy El-Din, N. M.; Sabaa, M. W. *Polym Degrad Stab* 1995, 47, 283.
- Behr, R. A.; Minor, J. E.; Linden, M. P.; Vallabhan, C. V. G. *J Struct Eng* 1984, 111, 1037.
- Vallabhan, C. V. G.; Das, Y. C.; Magdi, M.; Asik, M.; Bailey, J. R. *J Struct Eng* 1993, 119, 1572.
- Vallabhan, C. V. G.; Minor, J. E.; Nagalla, S. R. *J Struct Eng* 1987, 113, 36.
- Huntsberger, J. R. *J Adhes* 1981, 13, 107.
- David, D. J.; Wittberg, T. N. *J Adhes* 1984, 17, 1231.
- Sha, Y.; Hui, C. Y.; Kramer, E. J.; Garrett, P. D.; Knapczyk, J. W. *J Adhes Sci Technol* 1997, 11, 49.
- Decker, C.; Moussa, K. *J Appl Polym Sci* 1995, 55, 359.
- dos Reis, H. L. M. *Br J Non-Destructive Testing* 1993, 35, 565.
- Jandeleit, O. *Glastech (Ber)* 1989, 62, 204.
- Shabanova, E. B.; Kaprov, A. I.; Pavlyukova, G. V. *Glass Ceram* 1987, 44, 227.
- Timmermann, A. *Proceedings of the Conference on Vision in Vehicles*, Nottingham, UK, September 9–13, 1985, 331.
- Wong, B. C. *Glass Processing Days, Proceedings of the 5th International Conference on Architectural and Automotive Glass*, Tampere, Finland, September 15–19, 1997, 464.